Atom Trap Trace Analysis of Calcium Isotopes

Hoekstra, Steven

Chapter 2

Laser Cooling and Trapping of Calcium

2.1 Introduction

In this chapter the most relevant principles for understanding the cooling and trapping of calcium isotopes will be introduced. After a general introduction on the alkaline-earth atoms and the isotopes of calcium in sections 2.1.1 and 2.1.2 the atomic structure of both the odd and even isotopes of calcium is treated (section 2.2). In section 2.3 the implications of the atomic structure for laser cooling are discussed. In the last section some applications of the cooling principles are treated: transverse atomic beam cooling, beam slowing, beam deflection and magneto-optical trapping.

2.1.1 Alkaline-earth atoms

Alkaline-earth atoms are the atoms of the second column of the periodic system of the elements. Their electronic structure is characterized by a closed outer shell of two *s* electrons. Calcium has twenty electrons: the electronic configuration is that of argon plus two electrons outside the filled 3p shell, $[Ar]4s^2$. After the trapping of most alkali atoms (hydrogen, lithium, sodium, potassium, rubidium, cesium and francium), attention has been paid to the cooling and trapping of the alkaline-earths. Five years after demonstrating the first Magneto-Optical Trap for sodium by Raab *et al* [68] calcium was trapped for the first time in 1992 by Kurosu and Shimizu [73]. Other members of the alkaline-earth atom group are beryllium, magnesium, strontium, barium and radium. These atoms share some interesting properties for cold atom research. The spin-forbidden intercombination lines between the singlet and triplet system have very narrow linewidths, and are therefore studied for use in ultra-precise atomic clocks [74–76]. The ground-state of the even isotopes has zero nuclear spin and in most cases there is a strong resonance transition, suitable for cooling, from the $^1S_0$ ground state to the $^1P_1$ excited state.

Table 2.1: *Properties of the calcium isotopes. Shown are the relative natural abundance, the nuclear spin, the half-life time and for the stable isotopes the isotope shift of the cooling transition relative to ^{40}Ca in MHz. The shifts given for ^{41}Ca and ^{43}Ca are for the 9/2, 7/2 and 5/2 hyperfine components respectively*

Isotope	*Rel. nat. abundance*	*Nucl. spin*	*Half-life*	*Isotope-shift (MHz)*
39	-	$3/2$	859.6 ms	
40	0.9694	0	stable	0
41	$1 \cdot 10^{-14}$	$7/2$	103,000 yrs	$154/248/303$
42	0.0065	0	stable	393
43	0.0014	$7/2$	stable	$554/633/675$
44	0.0209	0	stable	774
45	-	$7/2$	162.61 d	
46	0.00004	0	stable	1160
47	-	$7/2$	4.536 d	
48	0.0019	0	$6 \cdot 10^{18}$ yrs	1513
49	-	$3/2$	8.718 m	

2.1.2 Calcium isotopes

By far the most abundant isotope of calcium is ^{40}Ca, as can be seen from table 2.1 in which isotopic properties of relevance for this research are shown. By far the least abundant natural isotope is ^{41}Ca. In the following sections the electronic structure of the calcium isotopes will be discussed. Only the odd isotopes have a nuclear spin. This is explained in section 2.2.3. The presence of the nuclear spin has some important consequences for the electronic structure, and therefore also for the cooling and trapping of the odd isotopes. Besides the difference in the electronic structure due to the spin of the nucleus there is the isotope shift of the levels, mostly due to the mass of the nucleus. The resulting differences in the frequency of the cooling transition are summarized in figure 2.1.

2.2 Electronic structure of the calcium isotopes

Since for the even isotopes the nuclear spin is absent, first the electronic structure of the even isotopes will be considered. The electronic structure of the even isotopes is different only because of the isotope shift, treated in the next section. Then we will discuss the nuclear spin of the odd isotopes, and show how that influences the electronic structure. Finally the interaction of an external magnetic field with both even and odd isotopes will be discussed.

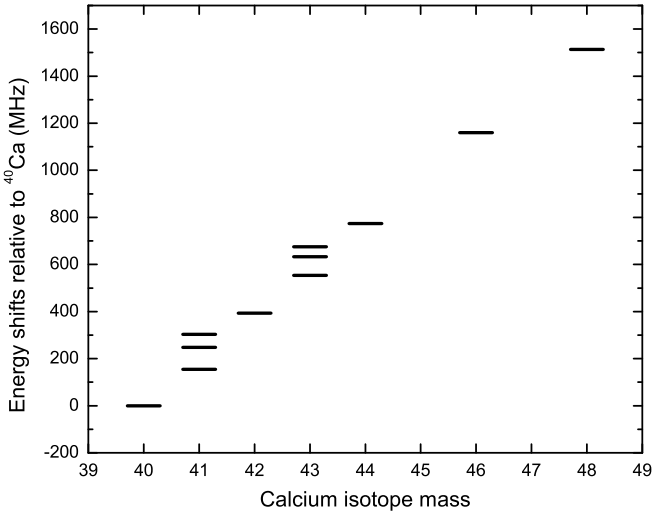

Figure 2.1: *The energy shifts of the excited state of the cooling transition for the different isotopes relative to ^{40}Ca. For the odd isotopes the three hyperfine components are shown*

2.2.1 The even calcium isotopes

Instead of giving a complete treatment of the electronic structure of calcium from first principles (which can be found in many textbooks e.g. [77]) here only a short summary will be given, focussing on the most important implications for laser cooling and trapping.

The spins of the two valence electrons can be aligned either parallel or antiparallel. Therefore the different terms can be split in a singlet system and a triplet system. In the singlet system the spins of the two electrons are aligned anti-parallel, therefore the total spin S=0. For parallel aligned electrons the total spin is S=1. The most relevant energy levels are shown in the Grotrian diagram in figure 2.2. The transition from the ground state ($4s^2\ ^1S_0$) to the ($4s4p\ ^1P_1$) state, corresponding to a wavelength of 423 nm, has the largest transition rate. This transition is well suited for laser cooling because of the high transition rate ($2.18 \cdot 10^8$ /s) and the large photon energy (2.7 eV).

2.2.2 Isotope shifts

The difference in the composition of the nucleus for two isotopes of an element influences the energy levels of the atom: this can be detected as a shift in the resonance energy (or frequency) of a given electronic transition. A measurement of this isotope shift is actually a very useful tool to learn about the nuclear structure. The measured isotope shift of a particular optical transition is the sum of a shift due to the change in mass of the nucleus and of a shift resulting from the variation of the nuclear charge radius (the volume effect) [78]. The mass shift can further be separated into a normal mass shift coefficient and a

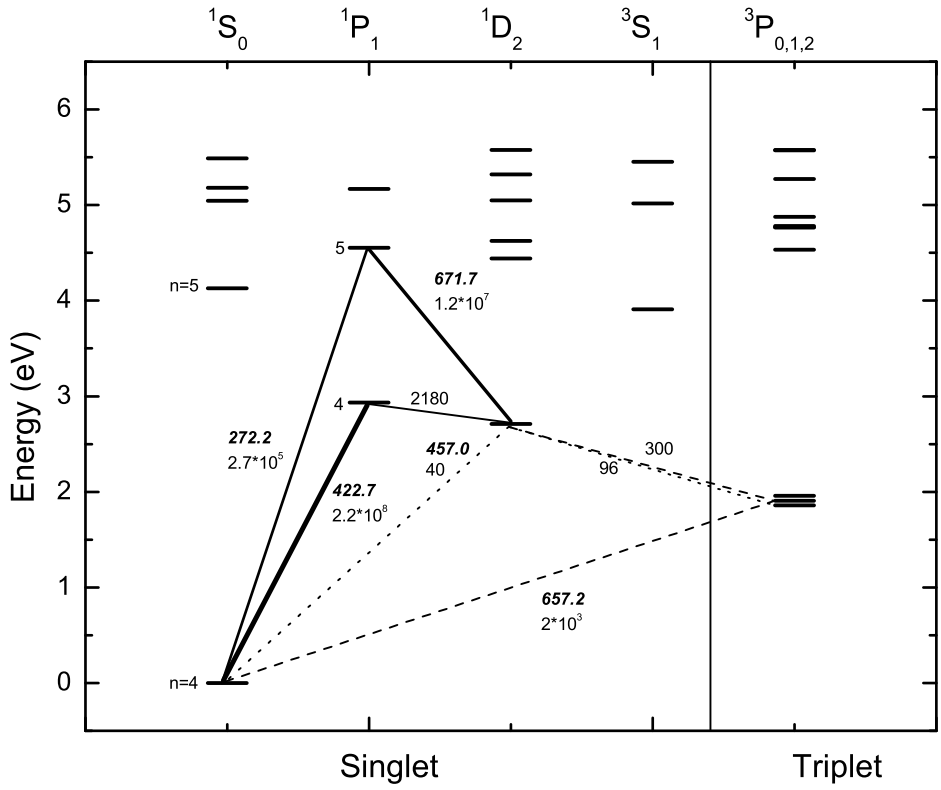

Figure 2.2: *A Grotrian diagram showing some of the most relevant states of the ^{40}Ca atom. The singlet and the triplet system can be seen. Wavelengths of the most relevant transitions are given in nm (upper number), as well as the transition rates in s^{-1}. The thickness of the connecting lines indicates the strength of the transition. Only very weak transitions are possible between the singlet and the triplet system*

specific mass shift coefficient. The normal mass shift coefficient can easily be calculated. The specific mass shift is due to the interactions (correlations) between the different outer electrons, and can not be calculated easily. For light nuclei such as calcium, the mass effect dominates, and the volume effect and the nuclear structure effects contribute as a rule less than 10% of the total shift. The isotope shifts of the cooling transition for the various isotopes of calcium are given in table 2.1. These shifts have been measured most accurately by Nörtershäuser *et al* in 1998 [78].

2.2.3 Nuclear spin

The nuclear spin of the calcium isotopes can be explained by the independent particle or shell model of the nucleus. In the independent particle model [79] we find that in the case of ^{40}Ca all levels up to the the $1d_{3/2}$ level are completely filled by the 20 neutrons. When we add another neutron the next shell is populated. The resulting total angular momentum for a nucleon with intrinsic spin $s = (1/2)\hbar$ in an orbit **l** with total angular momentum **j**=**l**+**s** is $l \pm 1/2$. The next available level is the $1f_{7/2}$ level; so the resulting nuclear spin of any odd number of neutrons up to ^{47}Ca is 7/2. The two neutrons of the even isotopes pair up in an antiparallel configuration with a resulting 0 nuclear spin. With ^{48}Ca we reach another completely filled shell: adding more neutrons will populate the next level, $2p_{3/2}$, resulting in a 3/2 nuclear spin. Removing a neutron from the closed $1d_{3/2}$ shell of ^{40}Ca, ending up with ^{39}Ca, also results in a net nuclear spin of 3/2.

2.2.4 The odd calcium isotopes: hyperfine structure

In first order, the IJ coupling can be described by a magnetic dipole interaction and an electric quadrupole interaction. For a particular hyperfine sublevel, identified by the hyperfine quantum number F, the energy shift induced by both effects is given by the Casimir formula [80]

$$\Delta E_F = \frac{A}{2}C + \frac{B}{4}\frac{3C(C+1)/2 - 2I(I+1)J(J+1)}{(2I-1)(2J-1)IJ} \tag{2.1}$$

where A is the magnetic dipole coupling constant, also called the hyperfine structure constant, B is the electronic quadrupole constant and C is composed from the state quantum numbers as

$$C = F(F+1) - J(J+1) - I(I+1)$$

For ^{41}Ca the isotope shifts and hyperfine splitting have been measured [78], from which A and B can be calculated. The values found for ^{41}Ca are an isotope shift of 221.8 MHz, $A = -18.58$ MHz, $B = -5.1$ MHz and $I = \frac{7}{2}$. For the excited 4s4p $^1P_1$ term $J = 1$, which means that $F = \frac{5}{2}, \frac{7}{2}, \frac{9}{2}$. The energy shifts with respect to ^{40}Ca, including the isotope shift, are

$$\begin{aligned} \Delta E_{9/2} &= 154 \\ \Delta E_{7/2} &= 248 \\ \Delta E_{5/2} &= 303 \end{aligned} \tag{2.2}$$

For the ground state $J = 0$ and so $F = 7/2$ ([77], [78]). The situation is similar for ^{43}Ca, where the following energy shifts with respect to ^{40}Ca are found:

$$\begin{aligned} \Delta E_{9/2} &= 554 \\ \Delta E_{7/2} &= 633 \\ \Delta E_{5/2} &= 675 \end{aligned} \tag{2.3}$$

2.2.5 Interaction with an external magnetic field

Depending on its strength, an external applied magnetic field (B_0) interacts with the total or the individual magnetic moments. The resulting shift of the interaction energy is the Zeeman effect.

The simplest case is that of the even isotopes, where the nuclear spin is absent. This state has L=1, S=0. The interaction energy is given by

$$V_{mj} = -\overrightarrow{\mu_J} \cdot \overrightarrow{B} = g_J \mu_B m_J B \tag{2.4}$$

In this equation the fine-structure Landé g-factor is introduced,

$$g_J \;=\; 1 + \frac{J(J+1) + S(S+1) - L(L+1)}{2J(J+1)} \tag{2.5}$$

In the case of the ^{1}P$_1$ state $L = J$ so $g_J = g_L = 1$. The result is a linear shift of the energy with magnetic field. The magnitude of the shift can be calculated from the values of g_J and μ_B and is $\pm$ 1.45 MHz / Gauss for the $m_J = \pm 1$ states.

For the odd isotopes the situation is more complex. Initially, for weak magnetic fields, the external magnetic field interacts with the magnetic moment of the total angular momentum

$$V_{HFS} = -\overrightarrow{\mu_F} \cdot \overrightarrow{B} = g_F \mu_B m_F B \tag{2.6}$$

In this equation the hyperfine-structure Landé g-factor g_F is introduced:

$$\begin{aligned} g_F \;=\; & g_J \left(\frac{F(F+1) + J(J+1) - I(I+1)}{2(F+1)} \right) \\ & - g_I \frac{m_e}{m_p} \left(\frac{F(F+1) + I(I+1) - J(J+1)}{2F(F+1)} \right) \end{aligned} \tag{2.7}$$

The result is a splitting for weak magnetic fields of each term into 2F+1 equidistant components.

If the external magnetic field B_0 is strong enough, the coupling between I and J is lifted and one speaks of the Paschen-Back effect of the hyperfine structure which is also called the Back-Goudsmit effect. The LS coupling is determined by the magnetic moments of the electrons and remains in effect. It is stronger than the IJ coupling which is determined by an electronic moment and a much weaker nuclear moment. The resulting energy shift of the hyperfine levels is given by

$$E_{m_J m_I} = g_J \mu_B m_J B + A_J m_J m_I - g_I \mu_N m_I B \tag{2.8}$$

The first term in this equation is the Zeeman splitting of the multiplet with quantum number J, while the second term splits Zeeman sub-level m_J into (2I+1) hyperfine components. If the field is strong enough, the effect of the external field on the nucleus is no longer negligible compared to internal field. Therefore the third term is included.

The region of the transition between the limiting cases of strong and weak fields is usually very difficult to calculate, and can only be approximated. For this process, a *Maple* program, adapted from a program written by T. Loftus [81] was used. Details of the program can be found in ref. [82] and will not be reproduced here. The resulting shifts of the states are shown in figure 2.3. As a function of the applied external magnetic field the three hyperfine states, corresponding to F=5/2, 7/2 and 9/2, are split. It can be seen that also the ground state is split, although the splitting is negligible compared to that of the excited state.

For comparison also the shift of the excited state of ^{40}Ca is shown. Important to note is that the slope of the ($F = 9/2$, $m_F = 9/2$) component of the excited state of ^{41}Ca is similar to the slope of the $m_J = 1$ component of the excited state of ^{40}Ca. The strength of the magnetic field required for trapping is thus similar for both odd and even isotopes.

2.2.6 Transition strengths

The final part of this section is devoted to the calculation of the transition strength of the cooling transition. It is important to know how the nuclear spin of the odd isotopes influences the transition strength within the hyperfine states of the odd isotopes. This is of relevance to laser cooling and trapping because of optical pumping effects that arise when using polarized light, for example in sub-Doppler cooling.

The transition strength is given by the square of the transition matrix element μ_{eg}, which consists of a radial and an angular part. The radial part is the same for all transitions between two terms in the ground state and the excited state, and is therefore only a numerical factor that determines the absolute value of the coupling (Wigner-Eckhardt theorem). For simplicity and because we are only interested in the relative strength of the coupling for the odd and even isotopes the radial part is omitted here.

For the even isotopes the angular part of the transition matrix element is given by

$$(-1)^{L'+S-M'_J}\sqrt{(2J+1)(2J'+1)}\times\left\{\begin{array}{ccc} L' & J' & S \\ J & L & 1 \end{array}\right\}\left(\begin{array}{ccc} J & 1 & J' \\ M_J & q & -M'_J \end{array}\right) \qquad (2.9)$$

where S is the spin quantum number, {} are Wigner 6j symbols and () are Wigner 3j symbols. The quantum numbers with an accent are quantum numbers of the excited state, the others of the ground state. The polarization of the light is indicated by q: $q = +1$ for σ^+ polarized light, $q = 0$ for linear polarized light and $q = -1$ for σ^- polarized light. For our simple ^{1}S$_0$ - ^{1}P$_1$ transition using σ^+ light the angular part of the transition matrix element is

$$(-1)^{(0)}\cdot\sqrt{3}\cdot\sqrt{1/3}\cdot\sqrt{1/3}=\frac{1}{3}\sqrt{3}$$

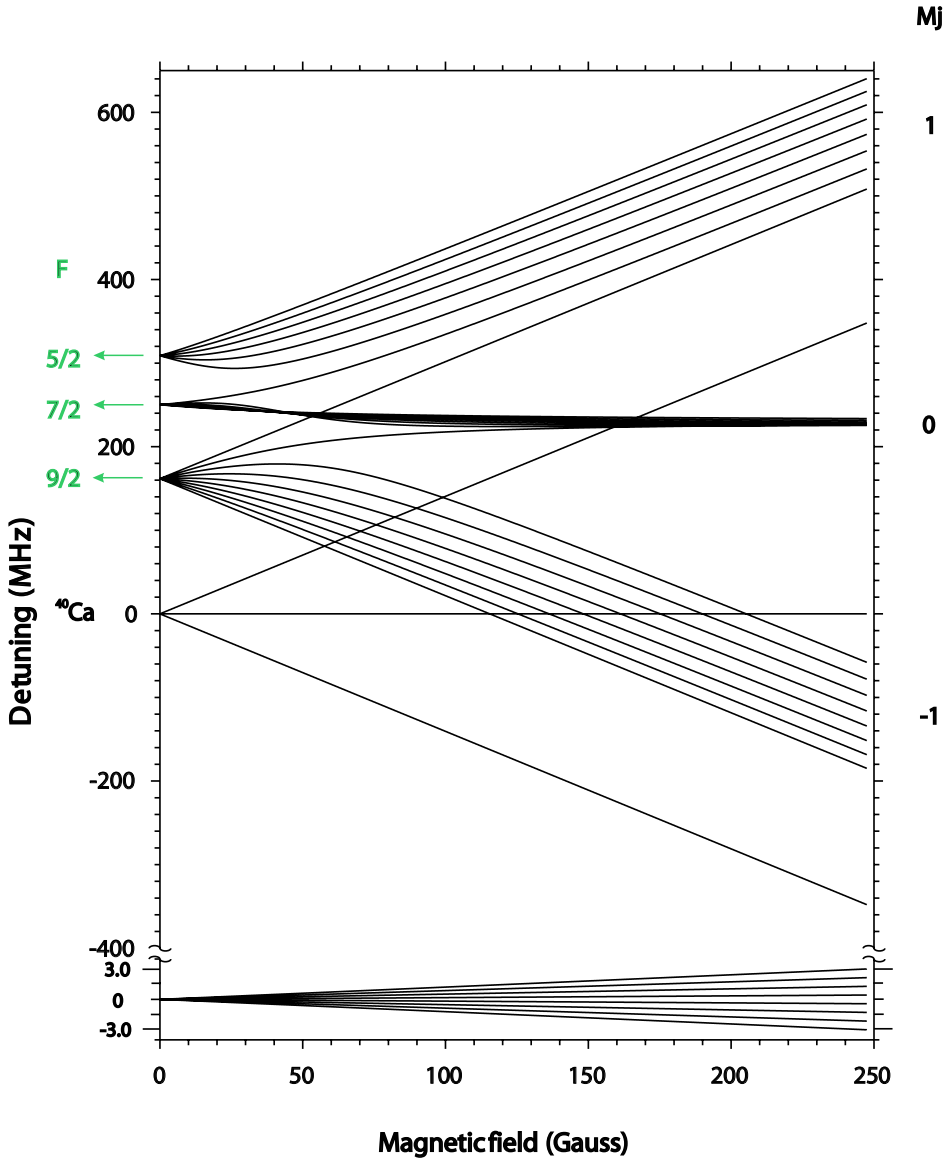

Figure 2.3: *The hyperfine Zeeman splitting of the* $^1S_0$-$^1P_1$ *transition of* ^{41}Ca *as a function of the applied magnetic field. The splitting is shown relative to* ^{40}Ca*. For comparison also the much simpler splitting of the excited state of* ^{40}Ca *is shown. In the lower part of the figure the scale of the splitting of the ground state of the odd-isotopes is plotted*

For the odd isotopes we have to include the nuclear spin, and the expression becomes

$$(-1)^{1+L'+S+J+J'+I-m'_F}\sqrt{(2J+1)(2J'+1)(2F+1)(2F'+1)} \times \begin{Bmatrix} L' & J' & S \\ J & L & 1 \end{Bmatrix} \begin{Bmatrix} J' & F' & I \\ F & J & 1 \end{Bmatrix} \begin{pmatrix} F & 1 & F' \\ M_F & q & -M'_F \end{pmatrix} \tag{2.10}$$

In figure 2.4 the calculated relative transition strengths are shown. They are multiplied by a factor of 252 to have all integer numbers. This scheme is the same for ^{43}Ca, ^{45}Ca and ^{47}Ca, because they have the same nuclear spin. Important to note is that the angular part of the transition matrix element for a transition in any of the odd isotopes from $m_F = 7/2$ to $m_F = 9/2$ is

$$(-1)^{(4)} \cdot \sqrt{240} \cdot \sqrt{1/3} \cdot -1/2\sqrt{1/6} \cdot -\sqrt{1/10} = \frac{1}{3}\sqrt{3}$$

and thus equal in strength to the transition in the even isotopes. This is important for the isotope selectivity that can be reached in the experiment, as will be discussed in chapter 4. The sum of the transition strengths for the 9/2, 7/2 and 5/2 states varies with $(2F+1)$. The ratio between the total transition strengths therefore is $10:8:6$.

2.3 Laser cooling theory

2.3.1 Interaction of light with atoms: saturation intensity

Consider a two level system with a ground state population N_1 and an excited state population N_2 such that the total population $N_1 + N_2 = 1$. The decay rate from the excited state to the ground state is given by Γ, and the corresponding lifetime of the excited state is given by $1/\Gamma = \tau$. A laser is tuned exactly to the resonance (detuning $\delta = 0$) with an intensity I. A saturation parameter s is defined as

$$s = 2\left(\frac{\Omega}{\Gamma}\right)^2 \equiv \frac{I}{I_s} \tag{2.11}$$

where Ω is the Rabi frequency. Here the saturation intensity I_s is introduced. This is the intensity at which the transition is power-broadened by a factor of $\sqrt{2}$. Its value depends on the details of the transition and is given by

$$I_s = \frac{\pi hc}{3\lambda^3\tau} \tag{2.12}$$

The excited state fraction is defined as

$$p \equiv \frac{N_2}{N_1+N_2} = \frac{1}{2}\frac{s}{1+s+(\frac{2\delta}{\Gamma})^2} \tag{2.13}$$

which for $I = I_s$ and $\delta = 0$ is $1/4$. In the limit of very high intensity ($I \gg I_s$) the maximum achievable population in the excited state is equal to the population of the ground state.

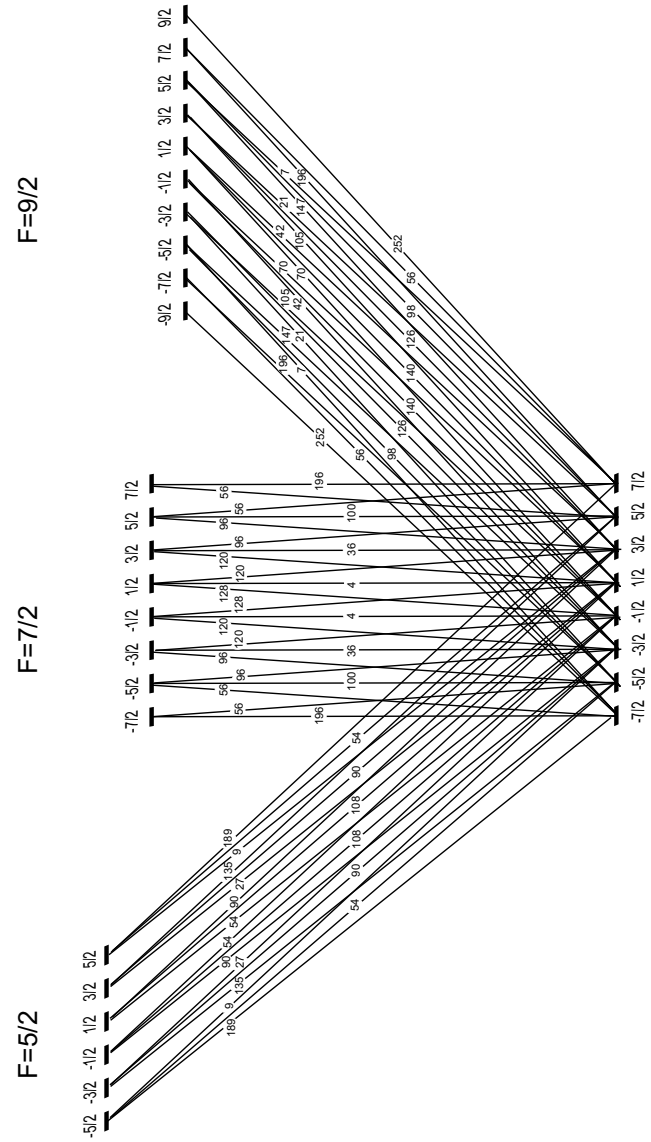

Figure 2.4: *The transition strengths between the excited state $^1P_1$ and the ground state $^1S_0$ for Ca-41, 43, 45 and 47. The strength is given in the smallest possible integer numbers*

2.3.2 Scattering rate and radiation pressure

A two-level atom scatters photons when it is illuminated by a laser tuned to an electronic transition. Momentum is transferred from the photons to the atom because of the asymmetry between the absorption and emission processes: the photons absorbed from the laser beam all come from the same direction while the emission of the photons by the atom has an angular distribution that is inversion symmetric, i.e. the same number of photons is emitted in a given direction and the opposite direction. The resulting momentum transfer is called radiation pressure and it is the principal force in laser cooling. The Doppler shift ω_D of a moving atom, the isotope shift δ_{IS} and the natural linewidth Γ of the transition together determine the effective scattering rate of a specific isotope. For a specific laser detuning Δ and power s the scattering rate γ_p [83] is given by

$$\gamma_p = \frac{s\Gamma/2}{1+s+(2(\Delta+\omega_D+\delta_{IS})/\Gamma)^2} \tag{2.14}$$

2.3.3 Optical Molasses and the spontaneous force

Consider a two-level atom with a frequency interval between ground and excited state of ω_0, irradiated by a laser beam of angular frequency ω and wavelength λ. The frequency width of the laser is assumed to be smaller than the natural width of the transition. The detuning of the laser from resonance is given by $\Delta = \omega - \omega_0$. An atom moving with velocity v in the direction of propagation of the laser sees the laser light frequency Doppler shifted down (red detuning) by $2\pi v/\lambda = kv$, for a total detuning of $\Delta - kv$. The excited state population decays to the ground state at a rate Γ; the strength of the laser-induced coupling between the ground and the excited states is characterized by the saturation intensity I_s. For light with a wavelength λ, the momentum carried by one photon is $h/\lambda = \hbar k$. The average force on an atom moving in the positive(+)/negative(-) direction is this momentum times the average rate of absorbing photons:

$$F_\pm = \pm\hbar k\frac{\Gamma}{2}\frac{s}{1+s+[2(\Delta\mp kv)/\Gamma]^2} \tag{2.15}$$

This force, often called the radiation-pressure force, scattering force, or the spontaneous force, is in the direction of propagation of the light. The upper(lower) sign refers to the force from the laser light propagating in the positive (negative) direction. The sign of the force depends on the laser detuning with respect to the excited state: for negative (red) detuning of a few times the natural linewidth the force is positive, for positive (blue) detuning the force is negative. Note that the maximum value of this force is $\hbar k\Gamma/2$ for $I/I_s \gg 1$. For calcium atoms irradiated by light resonant with the $4s^2\ {}^1S_0$ - $4s4p\ {}^1P_1$ transition ($\lambda = 423$ nm and $\Gamma = 34$ MHz) the acceleration corresponding to the maximum force is $2.6\cdot 10^6 \mathrm{m/sec}^2$. I_s for this transition is 59.9 $\mathrm{mW/cm}^2$.

One-dimensional classical optical molasses is formed when we consider two counter-propagating laser beams. The average force on the atom is given by $F_+ + F_-$. In the case of low intensity the two lasers act independently on the atoms such that we can neglect

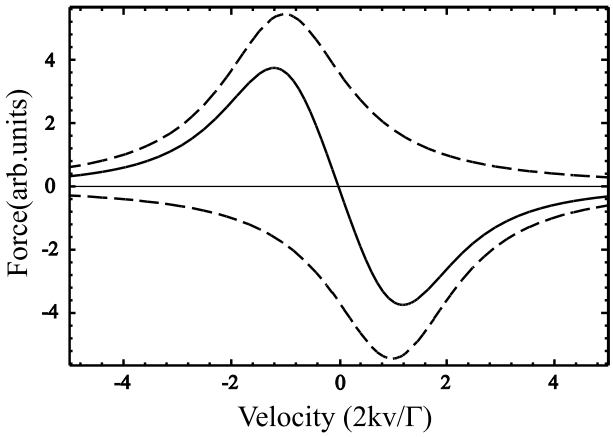

Figure 2.5: *The spontaneous force (equation 2.16) versus velocity. The dashed curves are the individual forces for each of the two counterpropagating beams, and the solid curve is the net force*

stimulated emission, power broadening or level shifts and we have for the total force

$$F = \frac{\hbar k\Gamma}{2}\frac{I}{I_s}\frac{kv}{\Gamma}\frac{16\Delta/\Gamma}{1+\frac{8}{\Gamma^2}(\Delta^2+k^2v^2)+\frac{16}{\Gamma^4}(\Delta^2-k^2v^2)^2} \tag{2.16}$$

It can be seen from this equation that the force is a product of the maximum radiation-pressure force, a normalized intensity, the ratio of the Doppler shift to the linewidth, and a factor depending on the detuning and the velocity. The spontaneous force, given by equation 2.16, is plotted in figure 2.5.

In the approximation that $|kv| \ll \Gamma$ and $|kv| \ll |\Delta|$ we have

$$F = 4\hbar k\frac{I}{I_0}\frac{kv(2\Delta/\Gamma)}{[1+(2\Delta/\Gamma)^2]^2} \tag{2.17}$$

For the case of the red-detuning the atoms see the laser beam opposing their motion Doppler shifted closer to resonance, so they absorb photons directed opposite their motion more often than photons directed along their motion. For $\Delta < 0$ this is a friction force, linear in v and opposing v. This damping force can be written as $F = -\alpha v$, where we have the damping coefficient

$$\alpha = 4\hbar k^2\frac{I}{I_s}\frac{(2\Delta/\Gamma)}{[1+(2\Delta/\Gamma)^2]^2} \tag{2.18}$$

The capture velocity $v_c = \Gamma/k$ is the velocity corresponding to the maximum force of the optical molasses, and depends on the linewidth of the transition used. For calcium on the cooling transition this velocity is 14.64 m/s [83], and the maximum acceleration is $2.6 \cdot 10^6$ m/s^2.

2.3.4 The Doppler limit

Atoms are not cooled to zero kinetic energy in optical molasses. There is a heating mechanism connected to the discrete momentum-steps that the atoms make during emission and absorption. Since the atomic momentum changes by $\hbar k$, the kinetic energy changes on the average by at least the recoil energy $E_r = \hbar^2 k^2/2M = \hbar\omega_r$. This means that the average frequency of each absorption is $\omega_{abs} = \omega_a + \omega_r$ and the average frequency of each emission is $\omega_{emit} = \omega_a - \omega_r$, where ω_a is the frequency of the laser light that was absorbed. Thus the light field loses an average energy of $\hbar(\omega_{abs} - \omega_{emit}) = 2\hbar\omega_r$ for each scattering. This loss occurs at a rate of $2\gamma_p$, and the energy is converted to atomic kinetic energy because of the recoil from each event. These recoils are in random directions, thus the atomic sample is heated.

The competition between heating and damping forces results in a steady state nonzero kinetic energy, $(\hbar\Gamma/8)(2|\Delta|/\Gamma + \Gamma/2|\Delta|)$. This energy has a minimum for a detuning of $\Delta = -\Gamma/2$. The temperature corresponding to the minimum of the kinetic energy is $T_D = \hbar\Gamma/2k_B$, which is called the Doppler temperature or the Doppler cooling limit. For ^{40}Ca this temperature is 831 μK, and it is the minimum temperature to which the calcium atoms can be cooled in optical molasses. For the odd isotopes more complicated cooling mechanisms might occur. The treatment of these so-called sub-Doppler cooling mechanisms is however beyond the scope of this thesis. More on sub-Doppler cooling in general can be found in [84, 85]. More specifically, the sub-Doppler cooling of alkaline-earth atoms is addressed in [86].

2.4 Laser cooling of atomic beams

2.4.1 Atomic beam compression

The transverse velocity of the atomic beam is determined by the exit channels of the oven: in our experiment these channels have a ratio of 1:10 (see section 3.4, resulting in a maximum transverse velocity which is about one tenth of the longitudinal velocity. The resulting divergence of the atomic beam is a major loss factor for the efficiency of the experiment.

By using optical molasses the transverse velocity component of the atoms can be reduced. Laser beams intersecting the atomic beam under an angle of 90° with a red detuning of $\sim 1\Gamma$ can reduce the transverse velocity component to the Doppler limit. The transverse velocity that can typically be cooled is up to 20 m/s with a few mW of laser light. The main reason for implementing a compression stage in an ATTA experiment is to increase the efficiency of the transfer of atoms from the oven to the trap.

2.4.2 Atomic beam deflection

The simplest method of deflecting an atomic beam is to irradiate it from one side with laser-light tuned to an atomic resonance. The resulting absorption and spontaneous emission of photons induces a radiation pressure that deflects the atoms. However, the draw-

backs of this simple method are large. If the interaction time is long enough the atoms will Doppler shift out of resonance, resulting in an impulse which is independent of transit time. However, even if all atoms receive the same impulse, the deflection angle is inversely proportional to the longitudinal momentum. It is therefore necessary to narrow the longitudinal velocity as much as possible to maintain a collimated deflected beam.

An alternative method for large angle deflection of an atomic beam, using a light field and keeping the **k** vectors always perpendicular to the atomic trajectory was proposed by Ashkin [87] and was realized with sodium atoms by Nellesen *et al* [88]. This method would work well for calcium atomic beams with velocities higher than $\approx$ 150 m/s: the longitudinal velocity on the desired circular orbit has to be large compared to the velocity corresponding with the natural linewidth of the cooling transition. Since the natural linewidth for calcium is rather large (34 MHz) this method is not well suited for calcium beams with velocities around 50 m/s.

The best option for the deflection of a slow calcium beam is a one-dimensional optical molasses [89] inclined by an angle α with respect to the atomic beam that damps the velocity components of the atoms in the direction of the lasers. This component is $v \cdot sin(\alpha)$ and has to be smaller than the capture velocity of the optical molasses. The possibility of large-angle deflection of a calcium beam has been shown by Witte *et al.* [66]. They deflected an estimated 10^{10} atoms/s over an angle of 30° with mean longitudinal velocities of 35 m/s and a velocity width of approximately 13 m/s. The transverse velocity of the deflected atoms was close to the one-dimensional Doppler limit.

In the Alcatraz experiment the deflection stage is an important step in the isotope selectivity, as is shown in chapter 4 and 5.

2.4.3 Atomic beam slowing

Because atoms can only be trapped in an Magneto-Optical Trap if they already move rather slow ($<$ 60 m/s) it is necessary for a high efficiency experiment to slow the thermal distribution of atoms down. When decelerating atoms with a counterpropagating beam tuned to a fixed frequency the atoms can only be slowed down over a relatively narrow velocity range. This is because the change in velocity will quickly be so large that they are no longer resonant with the slowing laser: the Doppler shift can be much larger then the natural linewidth of the transition. For the cooling transition in calcium the natural linewidth is 34 MHz; the Doppler shift is 2.4 MHz/m/s, so the velocity range over which deceleration can be reached in this fashion is only $\sim$ 15 m/s.

The solution to this problem was found in 1982 by Phillips and Metcalf [90], by introducing a so-called Zeeman slower. In a Zeeman slower a spatially varying magnetic field is applied so that the Zeeman shift compensates the Doppler shift as the atoms travel through the slower.

The changing Zeeman shift can be created by providing a magnetic field of the form

$$B(z) = B_b + B_0\sqrt{1 - z/z_0} \tag{2.19}$$

This form follows for a special case of constant deceleration. B_b is a bias field, that does not change as a function of z, $z_0 = Mv_0^2/\eta\hbar k\Gamma$ the length of the device, and we define

v_0 as the maximal initial velocity. η ($\eta < 1$) is a design parameter defined by $a = \eta a_{max}$ where a is the acceleration (which is negative in a Zeeman slower) and $a_{max} = \hbar k\Gamma/2M$. The maximum magnetic field B_0 is given by $B_0 = \hbar k v_0/\mu_B$.

The function of the bias field is the following. Most often the slow atoms are loaded directly in an atom trap from the exit of the Zeeman slower. To prevent the interaction of the slowing laser beam with the trapped atoms the slowing laser beam is shifted by ~ 10 linewidths in frequency. To maintain the resonance conditions the magnetic field is shifted accordingly using the bias field. If the bias field is chosen to be opposite in sign to the slowing field it also reduces the absolute value of magnetic field required.

Typical values for a calcium Zeeman slower are $a_{max} = 2.6 \cdot 10^6$ m/s^2, $B_0 = 1600$ Gauss (corresponding to a maximum slowing velocity of 1000 m/s), and a length of 0.4 - 1 meter. The length depends strongly on the laser power available and the capture velocity chosen. The final velocity of the atoms is typically 50 m/s, which can be chosen by tuning the frequency of the slowing laser.

2.5 Trapping

2.5.1 The Magneto-Optical Trap

Atoms can be trapped in a Magneto-Optical Trap (MOT) which consists of a combination of three orthogonal pairs of laser-beams (forming a 3D optical molasses) with a quadrupole magnetic field. The magnetic field is generated by a pair of coils in anti-Helmholtz configuration. The resulting magnetic field is zero in the center of the trap and increases in magnitude in all directions. The principle of the trapping force in a MOT is shown for a one-dimensional case in figure 2.6. A schematic drawing of the laser configuration and the magnetic field in three dimensions is shown in figure 2.7.

For calcium typically about 10^6 atoms can be trapped in a volume of 1 mm^3. The velocity distribution in the trap corresponds to a temperature of a few mK above absolute zero. The capture velocity of the trap depends on the magnetic field gradient and the laser detuning and power. A typical value is about 60 m/s for a (red) detuning of 55 MHz and a magnetic field gradient of 60 G/cm.

2.5.2 The average trapping time and trap loss mechanisms

The average time that a calcium atom remains trapped in the MOT is limited due to various loss mechanisms. We will discuss the various contributions to the loss in the following part of this chapter. The time evolution of the number of trapped atoms can be written as

$$\frac{dN}{dt} = R - \gamma N - \beta \int n^2(r) d^3r \tag{2.20}$$

where R is the atom capture rate, γ is the linear loss rate coefficient, β is the rate coefficient for two-body collisions and $n(r)$ is the number density. The linear loss from a calcium MOT is caused by two processes: the loss due to a 'leak' in the level structure

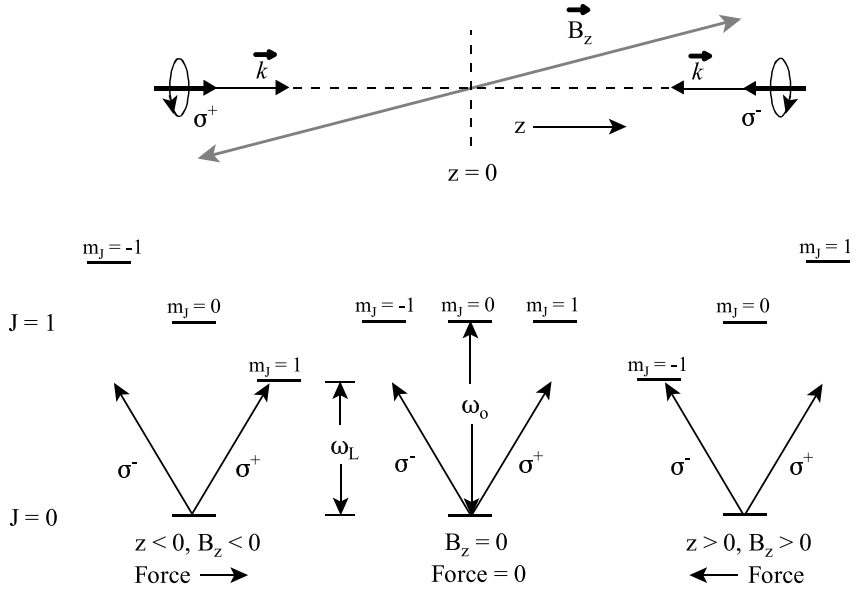

Figure 2.6: *Arrangement for a MOT in 1D. Because of the Zeeman shift of the atomic frequencies in the inhomogeneous magnetic field, atoms at the right are closer to resonance with the σ^--laser beam than with the σ^+ beam, and are therefore driven towards the center of the trap*

of calcium, and the loss due to collisions with the background gas. First we will examine the linear losses with the aid of a rate-equation model, taking into account the level structure of the calcium atom and the possibility to increase the average trapping time by using a repump-laser. Then we will analyze the effect of collisions between the trapped particles.

Rate equations

The average trapping time can be investigated by analyzing the system of coupled levels and transitions. Figure 2.8 illustrates the levels and transitions taken into account. This model is an extended version of the model developed by Grünert [91]. It is assumed that the strong trap laser radiation at 423 nm constantly excites atoms from the ground-state into the 4 ^{1}P$_1$ state, and therefore $N_2 = \varepsilon N_1$. The coupled differential equations for the populations are

$$\begin{aligned}
\dot{N}_1 + \dot{N}_2 &= R - (N_1 + N_2)\gamma + \Gamma_\eta N_3 + \Gamma_{61} N_6 - \Gamma_{23} N_2 \\
\dot{N}_3 &= \Gamma_{23} N_2 - (\Gamma_3 + \Gamma_{35} + W + \gamma) N_3 + \Gamma_{63} N_6 \\
\dot{N}_4 &= \Gamma_{34} N_3 - (\Gamma_{41} + \gamma) N_4 \\
\dot{N}_6 &= W N_3 - (\Gamma_{61} + \Gamma_{63} + \gamma) N_6
\end{aligned} \tag{2.21}$$

For brevity we use the substitution $\Gamma_3 = \Gamma_{31} + \Gamma_{34}$. Γ_η is the ^{1}S$_0$-population change due to transitions from ^{1}D$_2$ and ^{3}P$_1$. γ is the loss rate due to collisions or transitions into

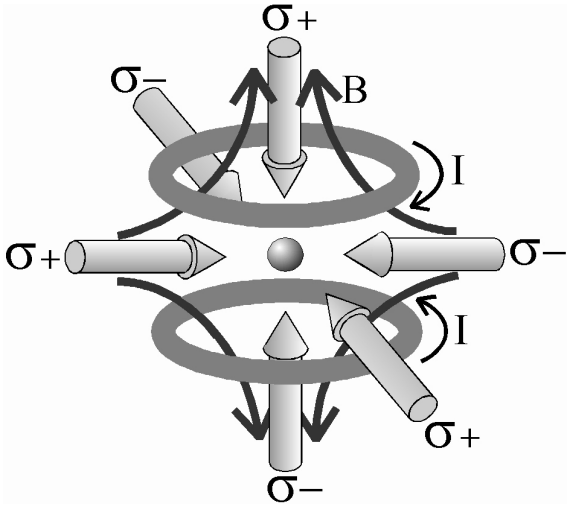

Figure 2.7: *Arrangement for a MOT in 3D, which consists of three pairs of counter-propagating laser beams, combined with the magnetic field generated by two coils in anti-Helmholtz configuration*

other levels than under investigation. W is the excitation rate due to the 672 nm laser, and these terms shall be neglected for the moment.

The rate equations can be summarized in

$$\frac{d}{dt}\begin{pmatrix} N_1 \\ N_3 \\ N_6 \end{pmatrix} = \mathcal{A}\cdot\begin{pmatrix} N_1 \\ N_3 \\ N_6 \end{pmatrix} + \begin{pmatrix} \frac{R}{1+\varepsilon} \\ 0 \\ 0 \end{pmatrix} \tag{2.22}$$

where

$$\mathcal{A} = \begin{pmatrix} -(\gamma+\Gamma_{23}\frac{\varepsilon}{1+\varepsilon}) & \frac{\Gamma_\eta}{1+\varepsilon} & \frac{\Gamma_{61}}{1+\varepsilon} \\ \Gamma_{23}\varepsilon & -(\Gamma_3+\Gamma_{35}+W+\gamma) & \Gamma_{63} \\ 0 & W & -(\Gamma_{61}+\Gamma_{63}+\gamma) \end{pmatrix} \tag{2.23}$$

In a first step we will look at the situation without the repump laser. Elimination of N_2 and neglecting the 672 nm laser leads to

$$\begin{aligned} \dot{N}_1 &= \tfrac{1}{1+\varepsilon}(R+\Gamma_\eta N_3) - (\gamma+\Gamma_{23}\tfrac{\varepsilon}{1+\varepsilon})N_1 \\ \dot{N}_3 &= \varepsilon\Gamma_{23}N_1 - (\Gamma_3+\Gamma_{35}+\gamma)N_3 \end{aligned} \tag{2.24}$$

The characteristic decay rates of the trap population are the eigenvalues of matrix $\mathcal{A}$. For this simpler situation $\mathcal{A}$ is a 2x2 matrix, and we find two eigenvalues

$$\lambda_\pm = -\frac{1}{2}(p\Gamma_{23}+2\gamma+\Gamma_3+\Gamma_{35}) \pm \frac{1}{2}\{[(p\Gamma_{23})-(\Gamma_3+\Gamma_{35})]^2+4p\Gamma_{23}\Gamma_\eta\}^{1/2} \tag{2.25}$$

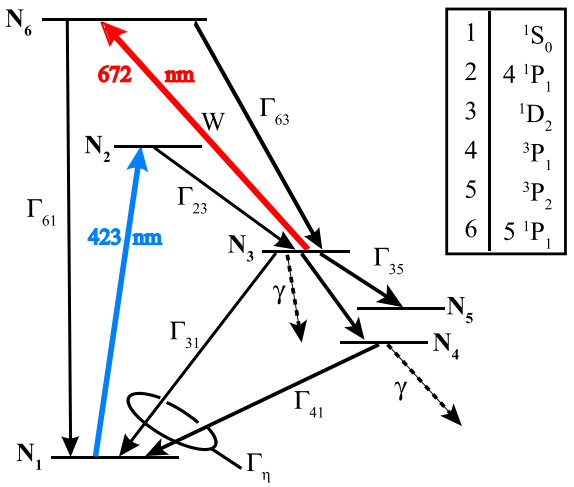

Figure 2.8: *Diagram of the levels and transitions relevant for the rate equation model*

i	1	2	3	4	5	6
assoc.level	$^1S_0$	$4\,^1P_1$	$^1D_2$	$^3P_1$	$^3P_2$	$5\,^1P_1$

i	2	3	4	6	2	6	3	3
j	1	1	1	1	3	3	4	5
Γ_{ij}/s^{-1}	$2.18\cdot10^8$	40	2100	$2.7\cdot10^5$	2180	$1.2\cdot10^7$	300	96

that correspond to the characteristic decay rates of the N_1 state and the N_3 state. Here we used the excited state fraction

$$p = \frac{\varepsilon}{\varepsilon+1} = \frac{N_2}{N_1+N_2} \tag{2.26}$$

In the steady state $\dot{N}_1 = \dot{N}_2 = \cdot N_3 = 0$, and thus

$$N_3 = \frac{p\Gamma_{23}R}{p\Gamma_{23}(\Gamma_{35}+\Gamma_3-\Gamma_\eta)+\gamma(\Gamma_{35}+\Gamma_3)} \tag{2.27}$$

$$N_1+N_2 = \frac{(\Gamma_{35}+\Gamma_3)R}{p\Gamma_{23}(\Gamma_{35}+\Gamma_3-\Gamma_\eta)+\gamma(\Gamma_{35}+\Gamma_3)} \tag{2.28}$$

The trap loading is terminated by switching off the slowing laser ($R = 0$). We will first neglect any losses due to collisions with the background gas ($\gamma = 0$). Furthermore, we will assume that the trapping beams are sufficiently large so that the atoms that diffuse away from the trap center while in state 3 ($^1D_2$) and 4 ($^3P_1$) can be recaptured ($\Gamma_3 = \Gamma_\eta$). Under these conditions, and for a typical excitation probability of $p = 1/6$, the

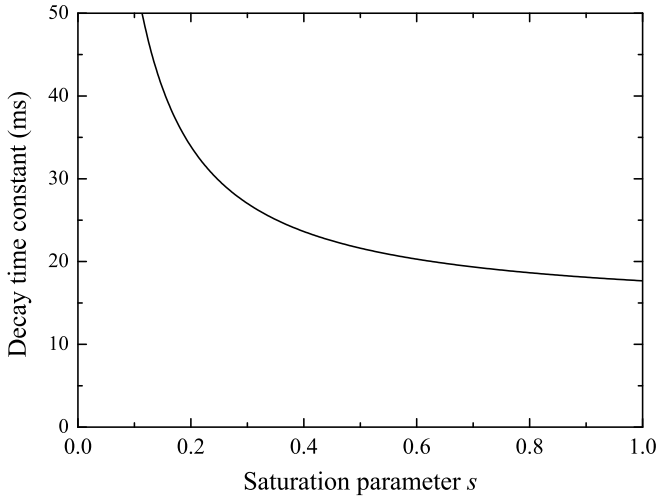

Figure 2.9: *The trap decay time constant as a function of the saturation parameter of the* 423 *nm laser*

characteristic decay rates for the N_1 and the N_3 state become

$$\lambda_{\pm} = \begin{cases} 47\ \mathrm{s}^{-1} \\ 753\ \mathrm{s}^{-1} \end{cases} \triangleq \begin{cases} 21.3\ \mathrm{ms} \\ 1.3\ \mathrm{ms} \end{cases}$$

The characteristic decay rate for the population in the N_1 state is equal to the trap decay time constant, which is the average trapping time.

In figure 2.9 the average trapping time is plotted as a function of the saturation parameter of the 423 nm laser for the case where the repump laser is off, and collisional losses are neglected. The saturation parameter is defined as the ratio between the intensity and the saturation intensity in equation 2.11. For low excitation rates the decay time constant increases, because the atoms are only lost from the trap after on average 100,000 excitations. It should not be concluded that the optimum trapping conditions exist for the lowest intensities: there is a minimum laser power required to keep the atoms trapped, and also the capture velocity of the trap decreases with decreasing laser power. A saturation parameter of $1/2$ corresponds to an excited state fraction of $1/6$.

In a next step we can include the parameter W, which is the excitation rate due to the 672 nm repump laser. Because atoms in the $^1D_2$ state are quickly pumped to the $5\ ^1P_1$ state from which they can decay to the ground state the average trapping time will increase. Shown in figure 2.10 is the trap decay time constant as a function of the excitation rate W by the repump laser. The maximum excitation rate (given by $\Gamma \cdot p$) of the 672 nm laser is $\Gamma_{63}/2 = 6 \cdot 10^6$ m/s^2. Therefore, the maximum achievable average trapping time is on the order of a few seconds: the leak can never be completely fixed.

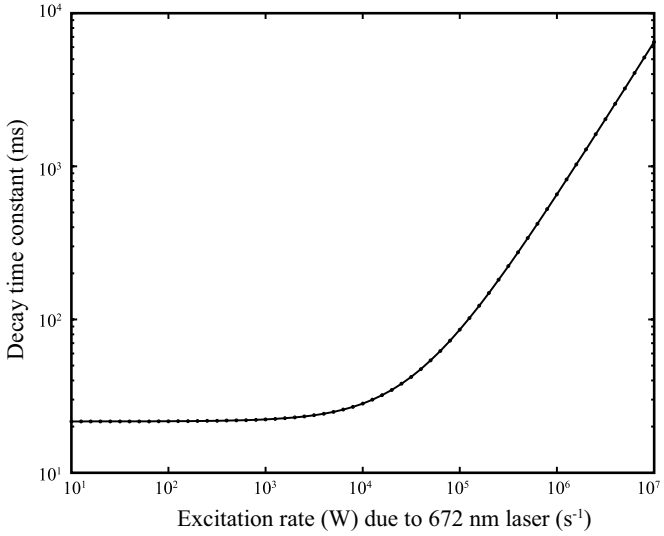

Figure 2.10: *The trap decay time constant as a function of the excitation rate by the* 672 *nm laser*

Assuming that we are able to saturate the repump transition, we can now study the effect of collisions with background gas, represented in the rate equation model by the parameter γ. First we set the following parameters fixed: $\varepsilon = 1/5$ (meaning that the excited state fraction is $p = 1/6$ and the saturation paramter $s = 1/2$) and $W = 6 \cdot 10^6$ s^{-1}. Now we can take a look at the decay time constant as a function of γ, shown in figure 2.11. In magneto-optical traps the loss rate due to collisions with the background gas can be calculated using a classical small-angle scattering approximation [92]. An atom will be lost from the trap if the speed due to the collision is $> v_0$ where $mv_0^2/2 = W_t$, with W_t the depth of the potential well of the trap. For trapped sodium atoms Bjorkholm [92] finds a scaling with the background pressure P (in mBar) which is in good agreement with experimental values of sodium traps: $\gamma = P/(2 \cdot 10^{-8})$. Typical pressures in our case are in the 10^{-9} to 10^{-8} range. The atomic radius for calcium and sodium is practically the same (190 pm for Sodium, 194 pm for calcium), but calcium is heavier, and therefore suffers less from the collisions with the background gas. Therefore we can use this formula to obtain an upper limit.

2.6 The statistics of a few trapped atoms

In this section the probability distribution of the photons emitted by a few trapped atoms is derived. This distribution can be used to fit the experimental data of single atoms, which will be reported on in chapter 5. After showing that the distribution of photons for a few trapped atom is poissonian, we will see that also the distribution of the number of trapped atoms is Poissonian. The inclusion of the distribution of the background photon

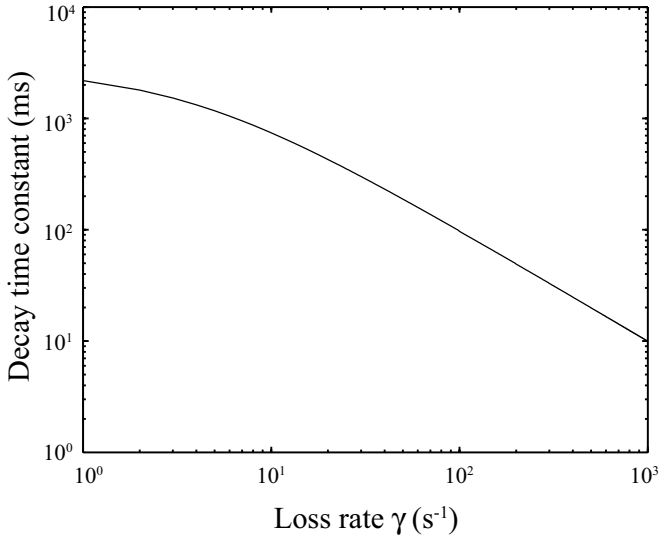

Figure 2.11: *The trap decay time constant as a function of the loss parameter γ, which is the loss due to collisions with background gas atoms*

counts is important because it is in magnitude comparable to the photons detected from the trapped atoms.

Statistics of the photons scattered by a few trapped atoms

The maximum possible scattering rate $\gamma_{\max}$ of a single atom is determined by the natural linewidth Γ, which is the inverse of the lifetime τ of the atomic transition.

$$\gamma_{\max} = \frac{\Gamma}{2} = \frac{1}{2\tau} \tag{2.29}$$

Thereby, we assume a two level system like it is encountered in all alkali systems. To avoid complication, we assume time intervals between subsequent photons which are in average much larger than the natural lifetime of the excited state. At this timescales the anti-bunching of the photons, which arises from the fact that an atom cannot scatter two photons simultaneously, can be neglected. Then, the probability of observing n photons in a time interval δt is given by the Poissonian distribution

$$p_{\mathrm{ph}}(1,n) = \frac{(n_{\mathrm{av}})^n}{n!}\, e^{-n_{\mathrm{av}}} \tag{2.30}$$

The argument "1" in $p_{\mathrm{ph}}(1,n)$ denotes that we are considering one atom. The mean number of photons is given by n_{av}. Note, that the distribution (2.30) is normalized:

$$\sum_{n=0}^{\infty} p_{\mathrm{ph}}(1,n) = 1 \tag{2.31}$$

and the expectation value is given by

$$\sum_{n=0}^{\infty} n p_{\mathrm{ph}}(1,n) = n_{\mathrm{av}}. \tag{2.32}$$

The mean number of photons n_{av} in the time interval δt already takes into account the scattering rate of the atom, the acceptance angle of the detection system and the efficiency of the photomultiplier. Although the distribution is still Poissonian a smaller value of n_{av} results in a deterioration of the signal to noise ratio which is given by $\sqrt{n_{\mathrm{av}}}$.

It can be shown that for two atoms in the trap the probabilities are again Poissonian distributed with a new mean value of twice the value for a single atom. Consequently, for k atoms, the probability of observing n photons is

$$p_{\mathrm{ph}}(k,n) = \frac{(k n_{\mathrm{av}})^n}{n!} e^{-k n_{\mathrm{av}}}. \tag{2.33}$$

Statistics of the number of atoms in the trap

The time dependent distribution of the number of atoms in the trap ($k(t)$) can be described (for low k) also by a Poisson distribution. This can be understood from a simple birth-death model (first applied to single atom statistics by Ruschewitz *et al* in 1996 [93]) which will be described in this section. Using this model to analyze the fluorescence signal of a few trapped atoms we can obtain information about the loading rate and the trap loss coefficient.

Since for very low atom numbers in the trap the intra-trap collisions become less and less important, we can set $\beta = 0$ in equation 2.20. This equation now simply becomes

$$\frac{dk}{dt} = R - \gamma k \tag{2.34}$$

Atoms enter the trap with a loading rate R and atoms leave the trap with a rate $\gamma = 1/\tau$, where τ is the average trapping time. The number of atoms in the trap at a time $t + \Delta t$ can be calculated from the number of atoms in the trap at time t if we know the transition probabilities for the transitions from k atoms in the trap to $k-1$, k and $k+1$ atoms in the trap as a function of Δt , which are given by

$$\begin{array}{ll} p_1(k \to k+1) & = R\Delta t \\ p_2(k \to k-1) & = \gamma k \Delta t \\ p_3(k \to k) & = 1 - (R + \gamma k)\Delta t \end{array} \tag{2.35}$$

The probability to find k particles in the trap at time $t + \Delta t$ is simply

$$P(k, t+\Delta t) = p_1 \cdot P(k+1,t) + p_2 \cdot P(k-1,t) + p_3 \cdot P(k,t) \tag{2.36}$$

We can now calculate the ratio

$$\frac{P(k,t+\Delta t) - P(k,t)}{\Delta t} \tag{2.37}$$

and if we let $\Delta t \to 0$ we obtain

$$\frac{\partial}{\partial t}P(k,t) = R \cdot P(k-1,t) + \gamma(k+1) \cdot P(k+1,t) - (\gamma k + R) \cdot P(k,t) \tag{2.38}$$

A stationary solution ($\frac{\partial}{\partial t}P(k,t) = 0$) is given by a Poisson distribution

$$P(k) = \frac{\langle k \rangle^k}{k!} e^{-\langle k \rangle} \tag{2.39}$$

with mean value of $\langle k \rangle = R/\gamma$ as follows from equation 2.34, and a variance $\langle k^2 \rangle - \langle k \rangle^2 = \langle k \rangle$.

Total statistics for photons

Now we are able to calculate the probability distribution for the photons, when the atom number is allowed to fluctuate around the mean value k_{av} according to equation (2.39). To do this we have to sum over all atom numbers and calculate the probability to get n photons multiplied with the probability to have k atoms:

$$p_{\mathrm{pa}}(n) = \sum_{k=0}^{\infty} p_{\mathrm{at}}(k) p_{\mathrm{ph}}(k,n). \tag{2.40}$$

At this point it is not possible (at least, it does not seem possible) to further simplify the sum (2.40). The only thing we can do is to rewrite the formula for numerical purposes as

$$p_{\mathrm{pa}}(n) = \frac{e^{-k_{\mathrm{av}}}(n_{\mathrm{av}})^n}{n!} \sum_{k=0}^{\infty} \frac{k^n (k_{\mathrm{av}} e^{-n_{\mathrm{av}}})^k}{k!}. \tag{2.41}$$

Including the background

So far we are able to describe photons arising from scattering of the atoms. In the following we will label these photons as "signal" photons. In every realistic setup, there is an additional contribution to the total count rate which comes from photons that are scattered from elements of the setup and subsequently detected by the photomultiplier. Especially for a small atom numbers these "background" photons have to be taken into account. We start with assuming again a Poissonian distribution for the background photons and write

$$p_{\mathrm{bg}}(n) = \frac{(b_{\mathrm{av}})^n}{n!} e^{-b_{\mathrm{av}}}. \tag{2.42}$$

We can now construct the total probability to detect n photons by summing over all possible combinations that the background photons (2.42) plus the signal photons (2.41) give a total number of n photons:

$$p(n) = \sum_{i=0}^{n} p_{\mathrm{bg}}(i) p_{\mathrm{pa}}(n-i). \tag{2.43}$$

This is the final result for the probability distribution of the number of photons for a low number of trapped atoms, including the background signal. It can be used to fit an experimentally obtained distribution of the number of photons, from which the average number of atoms in the trap can be extracted.

Correlation functions

More information can be obtained by looking at the time-correlation function of the fluorescence spectrum, which can be defined as

$$\langle N(t+\tau), N(t)\rangle_t = \langle N(t+\tau)\cdot N(t)\rangle_t - \langle N(t)\rangle_t^2 \tag{2.44}$$

For the underlying model of equation 2.38 the correlation function evolves as

$$\langle N(t+\tau), N(t)\rangle_t = \frac{R}{\gamma} e^{-\gamma t} \tag{2.45}$$

The value of the correlation function for $\tau = 0$, which is the variance, is equal to the mean number of trapped atoms, and the correlation time is equal to the trap lifetime. Using the time correlation signal from the fluorescence of a few trapped atoms we can therefore obtain from one measurement both the loading rate R and the trap loss coefficient γ.